Journal of Nuclear Medicine, published on August 17, 2017 as doi:10.2967/jnumed.117.192393

Response assessment of ^{68}Ga-DOTA-E-[c(RGDfK)]^2 PET/CT in lung adenocarcinoma patients treated with nintedanib plus docetaxel

AUTHORS
Oscar Arrieta[1]
Francisco O. Garcia-Perez[2]
David Michel-Tello[1]
Laura-Alejandra Ramírez-Tirado[1]
Quetzali Pitalua-Cortes[2]
Graciela Cruz-Rico[3]
Eleazar-Omar Macedo-Pérez[1]
Andrés F. Cardona[4,5]
Jaime de la Garza-Salazar[1]

AUTHOR DETAILS
[1] Thoracic Oncology Unit, Instituto Nacional de Cancerología (INCan), San Fernando #22, Sección XVI, Tlalpan, CP 14080, Mexico City, Mexico
[2] Department of Nuclear Medicine and Molecular Imagenology, Instituto Nacional de Cancerología (INCan), San Fernando #22, Sección XVI, Tlalpan, CP 14080, Mexico City, Mexico
[3] Laboratory of Personalized Medicine, Instituto Nacional de Cancerología (INCan), San Fernando # 22, Sección XVI, Tlalpan, CP 14080, Mexico City, Mexico
[4] Clinical and Translational Oncology Group, Clínica del Country, Bogotá, Colombia
[5] Foundation for Clinical and Applied Cancer Research – FICMAC, Bogotá, Colombia

CORRESPONDING AUTHOR

Oscar Arrieta, M.D. Head of Thoracic Oncology Unit and Laboratory of Personalized Medicine, Instituto Nacional de Cancerología (INCan), San Fernando # 22, Seccion XVI, Tlalpan, Mexico City, Mexico, CP 14080. Telephone: (+52) (55) 5628-0400, ext. 832, Fax (+52) (55) 551315-1223 Email: ogar@unam.mx

WORD COUNT 4991.

COMPETING INTERESTS

All authors confirm that they have no competing interests to declare.

FINANCIAL DISCLOSURES

This work was accepted to be presented as a poster at the 2016 World Conference on Lung Cancer in Vienna, Austria.

ACKNOWLEDGEMENTS

None

RUNNING TITLE
^{68}Ga-DOTA-RGD and nintedanib in NSCLC

ABSTRACT

Nintedanib is an oral angiokinase inhibitor used as second-line treatment for NSCLC. New radiotracers, such as ^{68}Ga-DOTA-E-[c(RGDfK)]^2, that target αvβ3 integrin might impact as a non-invasive method for assessing angiogenesis inhibitors.

Methods: From July 201 through October 2015, 38 patients received second-line nintedanib plus docetaxel. All patients underwent PET/CT with ^{68}Ga-DOTA-E-[c(RGDfK)]^2 radiotracer and blood-sample tests to quantify angiogenesis factors (FGF, VEGF and PDGF-AB) prior to and after completing 2 therapy cycles.

Results: Of the 38 patients, 31 had available baseline and follow-up PET/CT. Baseline LTV addressed with ^{68}Ga-DOTA-E-[c(RGDfK)]^2 PET/CT correlated with serum VEGF levels, while the baseline Lung/Liver SUVmax-Index correlated with PDGF-AB. After treatment, the ORR and DCR were 7.9% and 47.3%, respectively. A greater decrease in the LTV (-37.2% vs. -27.6%) was associated with a better DCR in patients (p=0.005). Median PFS was 3.7 months. Non-smokers and patients with a higher baseline LTV were more likely to have a higher PFS (6.4 vs. 3.74; p=0.023 and 6.4 vs. 2.1; p=0.003; respectively). OS was NR. Patients with a greater decrease in Lung SUVmax (NR vs. 7.1 months; p=0.016) and a greater decrease in the Lung/Spleen SUVmax Index (NR vs. 7.1; p=0.043) were more likely to have a longer OS.

Conclusion: ^{68}Ga-DOTA-E-[c(RGDfK)]^2 PET/CT is a potentially useful tool to assess responses to angiogenesis inhibitors. Further analysis and novel studies are warranted to identify patients who might benefit from this therapy.

KEYWORDS

adenocarcinoma, nintedanib/docetaxel, 68Ga-DOTA-E-[c(RGDfK)]^2, angiogenesis, αvβ3 integrin

INTRODUCTION

Lung cancer is the leading cause of cancer death worldwide (*1*). Most patients are diagnosed with advanced disease, and most patients treated with first-line platinum-based chemotherapy will progress after 3-7 months and require second-line therapy (*2*). Tumors grow by inducing endothelial proliferation to increase existing blood vessels to supply the tumor with oxygen and nutrients. Anti-angiogenic tyrosine-kinase-inhibitors have demonstrated a cytostatic effect on tumor cells by slowing growth and preventing development of distant metastases. Nintedanib, an oral angiokinase inhibitor targets the pro-angiogenic pathways mediated by vascular endothelial growth factor receptor 1–3, fibroblast growth factor receptor, and platelet-derived growth factor receptor α and β (*3,4*). Hypoxia is the most potent stimulus for their production by activating hypoxia-inducible factor–1α, which upregulates pro-angiogenic factors, resulting in rapid tumor growth (*5*). Vascular endothelial growth factor (VEGF) is the most studied and influential pro-angiogenic factor in the tumoral angiogenic process. Targeting VEGF has become relevant due to its potential for use of new drugs (*6*). Preclinical studies with nintedanib reported sustained blockade of vascular endothelial growth factor receptor 2 *in vitro* and tumor growth arrest (*3*). In phase 1/2 clinical trials, nintedanib showed a manageable safety profile and antitumor activity in patients with solid tumors, including non-small cell lung cancer (NSCLC) (*4,7*). The LUME-Lung 1 study demonstrated that patients with adenocarcinoma histology experienced significant improvement in median overall survival (OS) and progression-free survival (PFS) with nintedanib plus docetaxel *vs*. docetaxel alone. (*7,8*). Importantly, the subgroup of patients who progressed within 9 months after starting first-line therapy had a significantly longer OS, with a 3-month increase.

Integrins play a major role in adhesion of cells to extracellular matrix proteins. They are also responsible for regulating removal from the cell cycle and cell migration (*9*). The

αvβ3 integrin is a transmembrane protein constituting two subunits, α and β, and is generally expressed on mature endothelial and epithelial cells, as well as in tumor cells. It favors tumor growth of several angiogenesis-dependent tumors (*10*). The αvβ3 integrin can bind to the arginine-glycine-aspartic acid (RGD) amino acid sequence present in extracellular matrix proteins, such as vitronectin, fibrinogen and laminin (*11*). Due to this characteristic, αvβ3 integrin has been identified as a molecular target for non-invasive monitoring of malignant cells and treatment response assessment (*12,13*). Furthermore, Zannetti et al., using *in vivo* murine models, have shown that this peptide does not exhibit cross-reaction with αvβ5, which confers high selectivity in nuclear imaging (*14*). Recently, significant progress has been made in the development of new imaging techniques, such as ^{15}O-labeled radiotracers including oxygen-15 water and C^{15}O, which have been used to quantify tumor perfusion which might be related to angiogenesis. In parallel, αvβ3-targeting radiotracers for the visualization of αvβ3 expression in tumors by positron emission tomography/computerized tomography (PET/CT) have been synthesized, resulting in the use of the generator-produced radionuclide ^{68}Ga-DOTA-E-[c(RGDfK)]^2 (*10,13*). The application of ^{68}Ga-DOTA-E-[c(RGDfK)]^2 labeled peptides have attracted interest in cancer imaging because of their physical characteristics along with improved tumor targeting (*15,16*).

Anti-angiogenic therapy is a promising treatment for malignancies, including lung cancer. These are designed to inhibit tumor growth and dissemination instead of direct cytotoxicity, so they are unable to cause tumors to shrink rapidly in the short term making them difficult to evaluate by Computed tomography (CT) or ^{18}F-fluorodeoxyglucose PET/CT (*17*). However, the ^{68}Ga-DOTA-E-[c(RGDfK)]^2 peptide is a suitable ligand for the noninvasive visualization of αvβ3 expression *in vivo* that could provide information regarding molecular processes such as angiogenesis, and its correlation with chemotherapy response and prognosis (*10,13,15*). In the current study, we tested the ability of PET/CT with the

radiotracer ^{68}Ga-DOTA-E-[c(RGDfK)]^2 for assessing therapeutic responses to treatment with nintedanib plus docetaxel in lung adenocarcinoma. Furthermore, we evaluated the prognosis as determined by survival.

MATERIAL AND METHODS

Patients

This study was performed at the Instituto Nacional de Cancerología in Mexico City. All adult (>18 years) patients included had histologically confirmed stage IIIB/IV lung adenocarcinoma with failure after platinum-based first-line chemotherapy, an Eastern Cooperative Oncology Group performance status <2 and measurable disease according to Response Evaluation Criteria in Solid Tumors version 1.1.Patients with active brain metastases, who had received previous docetaxel, with recent history (<3 months) of clinically significant hemoptysis or a major thrombotic or clinically relevant major bleeding event in the past 6 months were excluded. All patients provided written informed consent. The study complied with the protocol and Declaration of Helsinki. The protocol was approved by an independent local ethics committee (015/007/ICI) (CEI/889/15).

Treatment Regimen

Patients received docetaxel 75 mg/m^2 on day 1 plus nintedanib 200 mg twice daily orally on days 2–21, every 3 weeks. Four cycles were given in combination, and then nintedanib was given alone as maintenance therapy. Nintedanib and docetaxel were provided by Boehringer Ingelheim as part of the Compassionate Use Program for nintedanib. Treatment was continued until disease progression or unacceptable toxicity. All patients were assessed for toxicities before starting each cycle according to the Common Terminology Criteria for Adverse Events (V-4.0).

Imaging

All patients underwent prior and after two cycles of treatment, ^{68}Ga-DOTA-E-[c(RGDfK)]^2 PET/CT using an mCT Excel 20 PET/CT scanner (Siemens, Erlangen, Germany) consisting of a bismuth osthosilicate full scanner and a 20-detector-row CT scanner. Whole-body CT was performed 40-50 minutes after injection of 188.7 MBq of ^{68}Ga-RGD (+/- 1.2), and transmission data were acquired using low-dose CT (120 kV, automated from 100-130 mA, a 512 × 512 matrix, a 50-cm field of view, 3.75-mm slice thickness, and a rotation time of 0.8 s), extending from the base of the skull to the proximal thighs. After CT acquisition, a whole-body PET was acquired in 3D (matrix 168× 168). For each bed position (16.2 cm, overlapping scale 4.2 cm), we used a 3-min acquisition time with a 15.5-cm field of view. The emission data were corrected for randoms, scatter and decay. Reconstruction was conducted with an ordered subset expectation maximization algorithm with 3 iterations/12 subsets and Gauss-filtered to a transaxial resolution of 6 mm at full-width at half-maximum. Attenuation correction was performed using low-dose non-enhanced CT. A workstation (Multimodality Workplace, Siemens) providing multi-planar reformatted images was used for image display and analysis. The median tumoral volume and the maximum standardized uptake value (SUVmax) of whole-body tumors were measured with the isocontour tool of the TrueD Syngo software (Siemens, Erlangen, Germany) using a threshold of 20% the SUVmax with manual adjustment.

Radiopharmaceutical Preparation

The synthesis of ^{68}Ga-DOTA-E-[c(RGDfK)]^2 was performed according to López-Rodriguez *et al*. (*16*)

PET/CT Interpretation Criteria

The ^{68}Ga-DOTA-E-[c(RGDfK)]^2 PET/CT scan was performed before starting treatment, a second scan was performed after two cycles of treatment. A negative PET/CT study was defined as tracer confined to normal uptake organs (spleen, urinary bladder, liver) and no other sites with uptake (*16,18*). A positive scan (progressive disease) was defined as at least one focus of abnormal intensity uptake, characterized by visual inspection and/or maximum SUVmax measurements. PET/CT images were visually analyzed by experienced nuclear medicine physicians.

Determination of Serum Angiogenesis Factors

Two serum samples were collected at baseline and after two therapy cycles. Serum levels were determined using Enzyme-Linked Immunosorbent Assay, which was performed according to the Quantikine human fibroblast growth factor (FGF), (VEGF) and platelet-derived growth factor-AB (PDGF-AB) immunoassay (DFB50, DHD00C, DVE00; R&D System, Minneapolis, MN, USA). All assays were performed in duplicate.

Outcomes

Primary endpoint was disease control rate (DCR) addressed by ^{68}Ga-DOTA-E-[c(RGDfK)]^2 PET/CT. Secondary endpoints included overall response rate (ORR), PFS, OS and toxicity profile. DCR was defined as the percentage of patients with advanced or metastatic NSCLC who have achieved complete response, partial response and stable disease to nintedanib plus docetaxel. ORR was defined as the the percentage of patients with advanced or metastatic NSCLC who have achieved complete and partial response to nintedanib plus docetaxel. PFS was defined as the time from treatment start to disease progression or death, and OS was defined as the period since beginning of treatment with nintedanib until the last follow-up or death.

Statistical Analysis

Continuous variables were summarized as means with standard deviations, categorical variables as frequencies and percentages. The Chi^2 or Fisher's exact tests were used to assess the significance among categorical variables. Patients were stratified on the DCR, and median values for PET/CT parameters were addressed by paired t-tests considering baseline and follow-up values. The percentage change (%Δ) was also calculated for baseline and follow-up PET/CT parameters.

Median OS and PFS were estimated using the Kaplan-Meier method. The median follow-up was 8.8 months (6.2 – 11.4). The log-rank test was used for comparisons among subgroups. A multivariate Cox-proportional hazard model was performed. All variables were dichotomized for the survival analyses. Statistical significance was determined as $p \leq 0.05$ using a two-tailed test. SPSS software version 21 (SPSS Inc., Chicago, IL) was used for all statistical analysis.

RESULTS

Study Design

Forty-six patients were assessed for eligibility; eight patients were excluded. Then, 38 patients underwent a PET/CT with ^{68}Ga-DOTA-E-[c(RGDfK)]^2 radiotracer scan. Five patients did not complete therapy due to unacceptable toxicity (n=1) or early disease progression (n=4). At the final follow-up, 33 patients were included, but 2 of them were excluded from the final analysis due to missing data (Fig1).

Characteristics of Patients

Among the 38 patients included, 16% of patients (6/38) had diabetes and 29% (11/38) had systemic hypertension at enrollment. Most patients had a good Eastern Cooperative Oncology Group performance status (<2) (97%; 37/38). Most common lung

adenocarcinoma histological subtypes were acinar (21%) and papillary (16%) First-line ORR and DCR were 47% (18/38) and 74% (28/38), respectively.

Treatment Characteristics

ORR and DCR of nintedanib plus docetaxel therapy were 8% (3/38) and 47% (18/38), respectively. When we analyzed the patients stratified on the DCR with nintedanib, we did not find differences among them by gender, median age, exposure to tobacco, diabetes, number of metastases, histological grade differentiation or median carcinoembryonic antigen. However, patients with systemic hypertension were associated with better DCR (77.8 vs. 22.2), although non-statistically significant (p=0.125).

Adverse Events

Only 34% (13/38) of patients presented severe adverse events requiring hospitalization. The most frequent adverse events were anemia (68%), nausea (66%), leucopenia (63%) and dyspnea (61%). The most common severe adverse events (graded ≥3) were neutropenia (21%), dyspnea (18%) leucopenia (16%) and asthenia (13%).

Assessment of ^{68}Ga-DOTA-E-[c(RGDfK)]^2 PET/CT Radiotracer

Figure 2 shows the therapeutic response to anti-angiogenic therapy. The ^{68}Ga-DOTA-E-[c(RGDfK)]^2 PET/CT scan prior to treatment shows intense avidity for the radiotracer in the right lung lesion and ipsilateral and contralateral mediastinal lymph nodes with an SUVmax of 7.6. The follow-up PET/CT shows significant reduction of avidity in the lung lesion and lymph nodes with a decreased SUVmax of 3.5 (Fig2).

Baseline, Follow-up and %Δ in ^{68}Ga-DOTA-E-[c(RGDfK)]^2 PET/CT Parameters and Angiogenic Factors

The assessment parameters of ^{68}Ga-DOTA-E-[c(RGDfK)]^2 PET/CT are shown in Tab1. Following treatment with nintedanib plus docetaxel, the parameters that showed a statistically significant reduction were the Lung/Spleen SUVmax Index (%Δ: -13%, *p*=0.022) and Lung Tumoral Volume (LTV) (%Δ: -38%; *p*=0.002). By contrast, the follow-up parameters that showed an increase after the anti-angiogenic therapy were FGF (%Δ: 125%; *p*=0.030) and PDGF-AB (%Δ: 70%; *p*=0.035) (Tab1).

^{68}Ga-DOTA-E-[c(RGDfK)]^2 PET/CT Parameters and Therapeutic Response to Nintedanib

PET/CT parameters stratified according to DCR showed that patients who did not achieve disease control had a higher and significant (*p*=0.008) %Δ reduction (-30%) in the Lung Tumor/Spleen SUVmax Index compared with patients who achieved a DCR (-13%, *p*=0.806). By contrast, patients who achieved a DCR had a higher and significant decrease in LTV (-37%, *p*=0.005) compared with patients who did not achieve a DCR, who had a lower and non-significant reduction in LTV (-28%; *p*=0.088). When we analyzed the patients regarding the %Δ the LTV assessed by Response Evaluation Criteria in Solid Tumors version 1.1 in relation to the %Δ in baseline lung tumor SUVmax assessed by ^{68}Ga-DOTA-E-[c(RGDfK)]^2 PET/CT, most of the patients who achieved a DCR had a decrease in the %Δ lung tumor SUVmax (Fig3).

^{68}Ga-DOTA-E-[c(RGDfK)]^2 PET/CT Parameters and Angiogenic Factors

When the relationship between ^{68}Ga-DOTA-E-[c(RGDfK)]^2 PET/CT parameters and angiogenic factors (FGF, VEGF, PDGF-AB) was analyzed, a positive correlation between the baseline Lung Tumor/Liver SUVmax Index and the baseline PDGF-AB was found (r-squared 0.418; *p*=0.030). Likewise, baseline LTV and baseline VEGF showed a positive correlation (r-squared 0.574; *p*=0.003).

Factors Associated with PFS and OS

The median PFS was 3.7 months. A greater baseline LTV (≥ 19.1 vs. <19.1) was associated with a higher PFS (6.4 vs. 2.1; *p*=0.007). (Fig4). In the multivariate analysis, systemic hypertension was associated with longer PFS (Hazard-ratio,95% Confidence-interval: 0.2 (0.1 – 0.80); *p*=0.021).

The OS was not reached (NR). A higher %Δ in the Lung Tumor SUVmax (≥-19% vs. <-19%) was associated with a higher OS (NR vs. 7.1, *p*=0.016). Patients with a higher baseline Lung Tumor/Spleen SUVmax Index (≥0.8 vs. <0.8) were more likely to have a longer OS (NR vs. 4.6 months; *p*=0.022). Moreover, a higher in the Lung Tumor/Spleen SUVmax Index (≥ -13% vs. <13%) was associated with a higher OS (NR vs. 7.8; *p*=0.043). (Fig4). In the multivariate analysis %Δ Lung tumor SUVmax associated with worse OS (Hazard-ratio,95% Confidence-interval: 3.1 (1.0 – 9.8); *p*=0.048).

DISCUSSION

Targeted therapies have changed treatment for lung cancer patients. Nevertheless, most will progress to chemotherapy alone. Anti-angiogenic agents have been studied in NSCLC with poor results. Bevacizumab, a monoclonal antibody against serum VEGF, improved prognosis in first-line settings in combination with paclitaxel or pemetrexed (*17,19*). NSCLC patients harboring an EGFR mutation have also shown a better PFS when treated with the combination of a tyrosine-kinase-inhibitor with bevacizumab. In the JO25567 trial, erlotinib plus bevacizumab improved PFS *vs.* erlotinib alone (16 vs. 9.7 months; Hazard-ratio: 0.054) (*17*).

Phase III studies in second-line therapy, such as ZODIAC (vandetanib ± docetaxel), ZEAL (vandetanib ± pemetrexed), and ZEST (vandetanib vs. erlotinib) tested the efficacy of anti-angiogenics, reporting limited impact in OS for advanced NSCLC patients (*20*).

Despite these results, there are two anti-angiogenic agents that show promise for improving OS after progression to first-line therapy: ramucirumab and nintedanib. Nintedanib is a triple angiokinase inhibitor targeting FGF, PDGF-AB and VEGF this last confers a poor prognosis in NSCLC at high serum levels (*21*). LUME-Lung 1 study, a phase III trial, improved survival rates at one (52.7 vs. 44.7%) and two years (25.7 vs. 19.1%) in first-line refractory patients, especially those with adenocarcinoma. This finding sets the base for biomarker correlation analyses and stratified treatment response assessment (*8*).

Potential biomarkers for angiogenesis have been studied, particularly with anti-VEGF antibodies (*22,23*). A phase 2/3 trial with carboplatin and paclitaxel with or without bevacizumab reported that low VEGF levels may predict a better PFS (p=0.04). Therefore, serum VEGF levels could potentially serve as a tool for identifying patients who might benefit from anti-angiogenic inhibitors.

Current need for early diagnosis, stratification and treatment response assessment has led to innovative techniques of nuclear medicine and molecular imaging. Medical imaging provides an advantage as a biomarker by being a noninvasive method that can provide different tumor information (*24*). Integrated PET/CT using ^{18}F-fluorodeoxyglucose the most widespread image radiotracer, can visualize tumor viability, anatomical structures of the tumor and surrounding normal tissues. Reported sensitivity, specificity and accuracy of ^{18}F-fluorodeoxyglucose PET/CT are 89%, 94% and 93%, respectively (*25*). However, it lacks tumor specificity, and has a poor uptake in tumor related neovascularization events (*18,26*). Thus, new approaches and optimal imaging methods must be established for new drugs, such as anti-angiogenic therapies.

An increased expression of αvβ3 integrin in tumoral endothelium as well as in tumor cells is associated with invasion and metastases (*27*). Furthermore, its two-subunit composition makes it a suitable, although not exclusive, receptor for the RGD sequence in the ^{68}Ga-DOTA-E-[c(RGDfK)]^2 radiotracer. In fact, other integrins (e.g. αvβ5, αvβ6) are related to RGD amino acid sequence binding (*28,29*). The αvβ3 integrin is targetable by various radiolabeled RGD peptides (*30*). Histologically, RGD peptides target tumor vasculature via RGD-integrin αvβ3 interaction with little extravasation. Therefore, decreased αvβ3 integrin expression measured by this imaging method can be associated with proper anti-angiogenic blockade (*28*). However, because tumor cells are also known to express several integrins, the overall uptake of a RGD peptide may very well be influenced by the expression of αvβ3, or other integrins, on the tumor tissue (*27*).

This study represents, to the best of our knowledge, the first nintedanib plus docetaxel therapy response in lung adenocarcinoma patients using ^{68}Ga-DOTA-E-[c(RGDfK)]^2 PET/CT as a surrogate biomarker and develops a prognostic model using dynamic molecular imaging. We demonstrate the relation between the angiogenic metabolic volume and the response to the multikinases inhibitor, which would be explained due to the relationship that exists between the RGD peptide uptake and the union to αvβ3 integrins. In this second-line study using a targeted agent with chemotherapy, we obtained survival rates (OS and PFS), therapy response rates (ORR and DCR) and the statistical correlations between the PET/CT parameters and clinical characteristics.

For the ORR and DCR assessment by PET/CT, results resemble the LUME-Lung 1 study, with no precedent of a tyrosine-kinase-inhibitor in combination with chemotherapy as second-line treatment response measurement using the ^{68}Ga-DOTA-E-[c(RGDfK)]^2 PET/CT scan. The main parameter used to assess ORR was tumor volume, which showed a

statistically significant reduction, mainly because of the metabolic decrease in target lesions after two cycles of nintedanib plus docetaxel therapy. There were also significant differences in the uptake rate in DCR between responders versus non-responders. Another important finding is that variations of Response Evaluation Criteria in Solid Tumors measurement and the Lung tumor SUVmax change rate seemed similar, which highlights that this study, one of the first of its class, could achieve the intended regulation for the use of a ^{68}Ga-DOTA-E-[c(RGDfK)]^2 PET/CT scan as a disease control monitoring method for anti-angiogenic drugs.

Additionally, when we assessed PFS, a higher baseline LTV was associated with a longer period until progression, which was consistent previous results (*16,31,32*). Thus, a higher targetable metabolic area might be associated with a higher tumor burden and therefore with a potentially higher treatment efficacy. We also observed that a higher percent decrease in the Lung Tumor SUVmax and in the Lung Tumor/Spleen SUVmax Index impacted OS but not PFS. These findings suggest a high correlation with therapeutic response to nintedanib. Our observations are consistent with a previous study investigating a ^{68}Ga-labeled pegylated RGD dimer (*28*). Validated by *ex vivo* immunohistochemistry, the authors found that the RGD radiotracer uptake was significantly reduced following anti-angiogenic therapy, reflecting tumor response significantly earlier than ^{18}F-fluorodeoxyglucose PET/CT. Contrary results were reported by Rylova *et al.* who studied ^{68}Ga-NODAGA-RGD for the *in vivo* monitoring of bevacizumab monotherapy in human squamous cell carcinoma xenografts in mice (*33*). Despite a reduced αvß3-integrin expression under VEGF inhibition, they observed an increased binding of ^{68}Ga-NODAGA-RGD in the investigated A-431 xenografts. Rylova *et al.* therefore concluded that the RGD radiotracer uptake might not reflect the changes in αvß3-integrin expression at the molecular level. They hypothesized that bevacizumab may activate αvß3-integrin, causing a higher affinity to ^{68}Ga-NODAGA-RGD and consequently increased radiotracer uptake *in vivo* (*33*).

Assuming a high-affinity state of αvß3-integrin however, one would expect an increased binding of the primary anti-αvß3-integrin antibody used in the immunohistochemical stainings and consequently false high αvß3-integrin levels. However, in line with our results, the authors found a reduced αvß3-integrin expression in the therapy group. In addition, VEGF is known to indirectly activate αvß3-integrin (*34*).

Our study has limitations, such as sample size and the relatively immature data employed for estimating OS. Nonetheless, it has the advantage of being the first prospective clinical-trial assessing the therapeutic response with ^{68}Ga-DOTA-E-[c(RGDfK)]^2, which in the future might also become a delivering radiotracer for refractory patients. Additionally, shows a high concordance with the LUME-1 study, a larger population-based clinical trial, and highlights a similar therapeutic response among Caucasian, Asian and Hispanic patients with adenocarcinoma treated with nintedanib plus docetaxel.

CONCLUSION

^{68}Ga-DOTA-E-[c(RGDfK)]^2 PET/CT is a potentially useful tool to assess responses to angiogenesis inhibitors. The present study may support the clinical basis for future studies investigating RGD-based hybrid imaging for monitoring therapeutic responses to molecular cancer therapies. RGD-based hybrid imaging may allow for a non-invasive real-time molecular typing of lung adenocarcinoma under anti-angiogenic treatment, adding complementary biomarkers of a therapeutic response to morphology-based and functional tumor response assessments.

REFERENCES

1. Ferlay J, Soerjomataram I, Dikshit R, et al. Cancer incidence and mortality worldwide: sources, methods and major patterns in GLOBOCAN 2012. *Int J Cancer.* 2015;136:E359-386.

2. Garon EB, Ciuleanu TE, Arrieta O, et al. Ramucirumab plus docetaxel versus placebo plus docetaxel for second-line treatment of stage IV non-small-cell lung cancer after disease progression on platinum-based therapy (REVEL): a multicentre, double-blind, randomised phase 3 trial. *Lancet.* 2014;384:665-673.

3. Hilberg F, Roth GJ, Krssak M, et al. BIBF 1120: triple angiokinase inhibitor with sustained receptor blockade and good antitumor efficacy. *Cancer Res.* 2008;68:4774-4782.

4. Mross K, Stefanic M, Gmehling D, et al. Phase I study of the angiogenesis inhibitor BIBF 1120 in patients with advanced solid tumors. *Clin Cancer Res.* 2010;16:311-319.

5. Kerbel R, Folkman J. Clinical translation of angiogenesis inhibitors. *Nat Rev Cancer.* 2002;2:727-739.

6. Gutierrez M, Giaccone G. Antiangiogenic therapy in nonsmall cell lung cancer. *Curr Opin Oncol.* 2008;20:176-182.

7. Reck M, Kaiser R, Eschbach C, et al. A phase II double-blind study to investigate efficacy and safety of two doses of the triple angiokinase inhibitor BIBF 1120 in patients with relapsed advanced non-small-cell lung cancer. *Ann Oncol.* 2011;22:1374-1381.

8. Reck M, Kaiser R, Mellemgaard A, et al. Docetaxel plus nintedanib versus docetaxel plus placebo in patients with previously treated non-small-cell lung cancer (LUME-Lung 1): a phase 3, double-blind, randomised controlled trial. *Lancet Oncol.* 2014;15:143-155.

9. Jin H, Varner J. Integrins: roles in cancer development and as treatment targets. *Br J Cancer.* 2004;90:561-565.

10. Garcia-Figueiras R, Padhani AR, Beer AJ, et al. Imaging of tumor angiogenesis for radiologists--part 1: biological and technical basis. *Curr Probl Diagn Radiol.* 2015;44:407-424.

11. Gasparini G, Brooks PC, Biganzoli E, et al. Vascular integrin alpha(v)beta3: a new prognostic indicator in breast cancer. *Clin Cancer Res.* 1998;4:2625-2634.

12. Kumar CC. Integrin alpha v beta 3 as a therapeutic target for blocking tumor-induced angiogenesis. *Curr Drug Targets.* 2003;4:123-131.

13. Ruoslahti E, Pierschbacher MD. New perspectives in cell adhesion: RGD and integrins. *Science.* 1987;238:491-497.

14. Zannetti A, Del Vecchio S, Iommelli F, et al. Imaging of alpha(v)beta(3) expression by a bifunctional chimeric RGD peptide not cross-reacting with alpha(v)beta(5). *Clin Cancer Res.* 2009;15:5224-5233.

15. van Hagen PM, Breeman WA, Bernard HF, et al. Evaluation of a radiolabelled cyclic DTPA-RGD analogue for tumour imaging and radionuclide therapy. *Int J Cancer.* 2000;90:186-198.

16. Lopez-Rodriguez V, Galindo-Sarco C, Garcia-Perez FO, Ferro-Flores G, Arrieta O, Avila-Rodriguez MA. PET-Based human dosimetry of the dimeric alphavbeta3 integrin ligand 68Ga-DOTA-E-[c(RGDfK)]2, a potential tracer for imaging tumor angiogenesis. *J Nucl Med.* 2016;57:404-409.

17. Barlesi F, Scherpereel A, Gorbunova V, et al. Maintenance bevacizumab-pemetrexed after first-line cisplatin-pemetrexed-bevacizumab for advanced nonsquamous nonsmall-cell lung cancer: updated survival analysis of the AVAPERL (MO22089) randomized phase III trial. *Ann Oncol.* 2014;25:1044-1052.

18. Vatsa R, Bhusari P, Kumar S, et al. Integrin avb3 as a promising target to image neoangiogenesis using in-house generator-produced positron emitter 68Ga-labeled DOTA-Arginine-Glycine-Aspartic Acid (RGD) ligand. *Cancer Biother Radiopharm*. 2015; 30(5):217-224.

19. Cardona AF, Rojas L, Wills B, et al. Pemetrexed/Carboplatin/Bevacizumab followed by maintenance Pemetrexed/Bevacizumab in hispanic patients with Non-Squamous Non-Small Cell Lung Cancer: Outcomes according to Thymidylate Synthase Expression. *PLoS One.* 2016;11:e0154293.

20. Morabito A, Piccirillo MC, Costanzo R, et al. Vandetanib: An overview of its clinical development in NSCLC and other tumors. *Drugs Today (Barc).* 2010;46:683-698.

21. Delmotte P, Martin B, Paesmans M, et al. [VEGF and survival of patients with lung cancer: a systematic literature review and meta-analysis]. *Rev Mal Respir.* 2002;19:577-584.

22. Dowlati A, Robertson K, Radivoyevitch T, et al. Novel phase I dose de-escalation design trial to determine the biological modulatory dose of the antiangiogenic agent SU5416. *Clin Cancer Res.* 2005;11:7938-7944.

23. Hanrahan EO, Ryan AJ, Mann H, et al. Baseline vascular endothelial growth factor concentration as a potential predictive marker of benefit from vandetanib in non-small cell lung cancer. *Clin Cancer Res.* 2009;15:3600-3609.

24. Baum RP, Kulkarni HR, Muller D, et al. First-In-Human study demonstrating tumor-angiogenesis by PET/CT Imaging with (68)Ga-NODAGA-THERANOST, a High-Affinity Peptidomimetic for alphavbeta3 Integrin Receptor Targeting. *Cancer Biother Radiopharm.* 2015;30:152-159.

25. Cai W, Niu G, Chen X. Imaging of integrins as biomarkers for tumor angiogenesis. *Curr Pharm Des.* 2008;14:2943-2973.

26. Haubner R, Wester HJ, Burkhart F, et al. Glycosylated RGD-containing peptides: tracer for tumor targeting and angiogenesis imaging with improved biokinetics. *J Nucl Med.* 2001;42:326-336.

27. Felding-Habermann B, Fransvea E, O'Toole TE, Manzuk L, Faha B, Hensler M. Involvement of tumor cell integrin alpha v beta 3 in hematogenous metastasis of human melanoma cells. *Clin Exp Metastasis.* 2002;19:427-436.

28. Shi J, Jin Z, Liu X, et al. PET imaging of neovascularization with (68)Ga-3PRGD2 for assessing tumor early response to Endostar antiangiogenic therapy. *Mol Pharm.* 2014;11:3915-3922.

29. DiCara D, Rapisarda C, Sutcliffe JL. Structure-function analysis of Arg-Gly-Asp helix motifs in αvβ6 integrin ligands. *J Biol Chem*. 2007;13:9657-9665.

30. Eo JS, Jeong JM. Angiogenesis Imaging Using (68)Ga-RGD PET/CT: Therapeutic Implications. *Semin Nucl Med.* 2016;46:419-427.

31. Kazmierczak PM, Todica A, Gildehaus FJ, et al. 68Ga-TRAP-(RGD)3 hybrid imaging for the in vivo monitoring of alphavss3-integrin expression as biomarker of anti-angiogenic therapy effects in experimental breast cancer. *PLoS One.* 2016;11:e0168248.

32. Withofs N, Signolle N, Somja J, et al. 18F-FPRGD2 PET/CT imaging of integrin alphavbeta3 in renal carcinomas: correlation with histopathology. *J Nucl Med.* 2015;56:361-364.

33. Rylova SN, Barnucz E, Fani M, et al. Does imaging alphavbeta3 integrin expression with PET detect changes in angiogenesis during bevacizumab therapy? *J Nucl Med.* 2014;55:1878-1884.

34. Byzova TV, Goldman CK, Pampori N, et al. A mechanism for modulation of cellular responses to VEGF: activation of the integrins. *Mol Cell.* 2000;6:851-860.

FIGURE AND TABLE LEGENDS

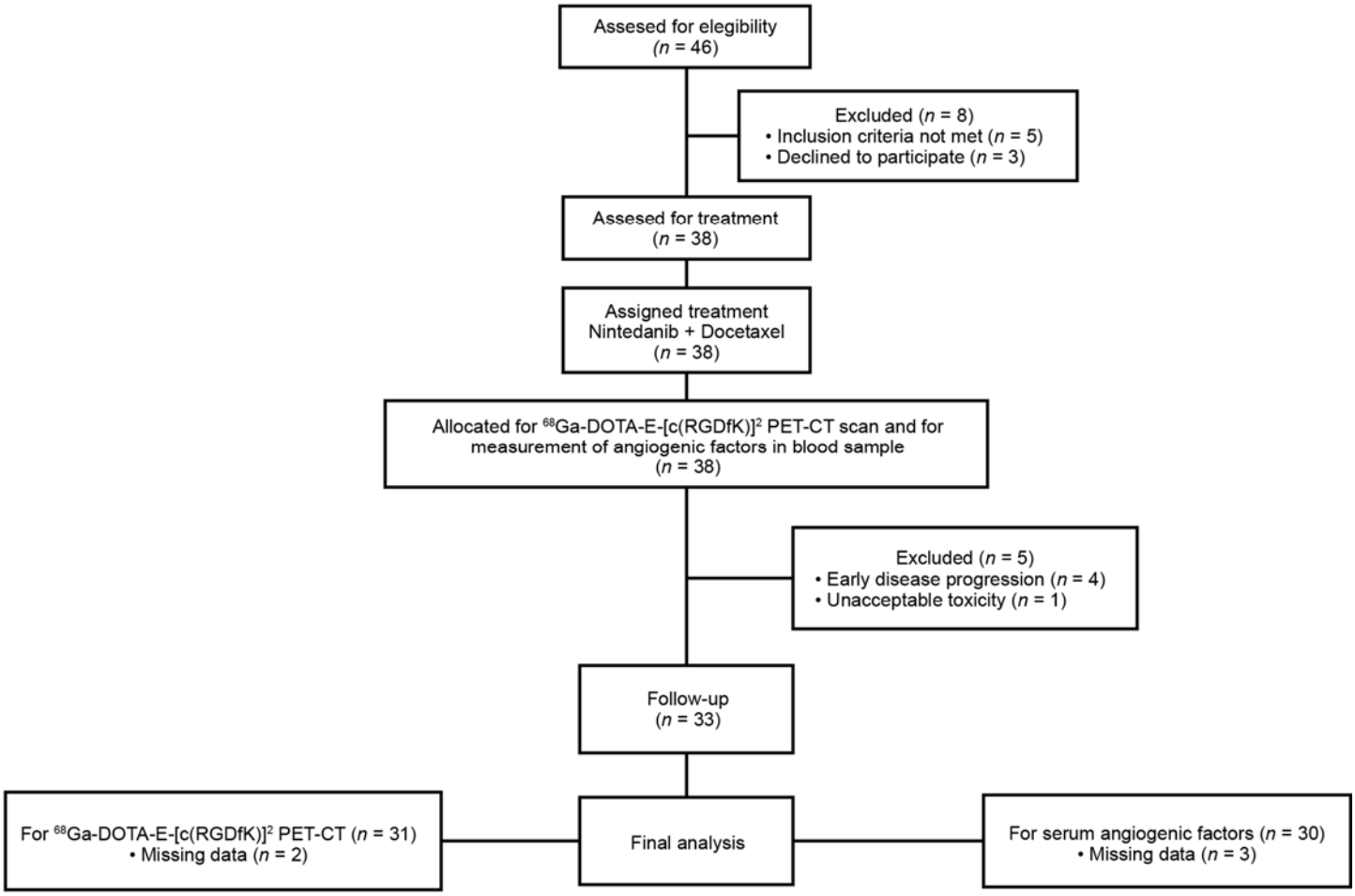

FIGURE 1. Flow diagram of patients included in the analysis

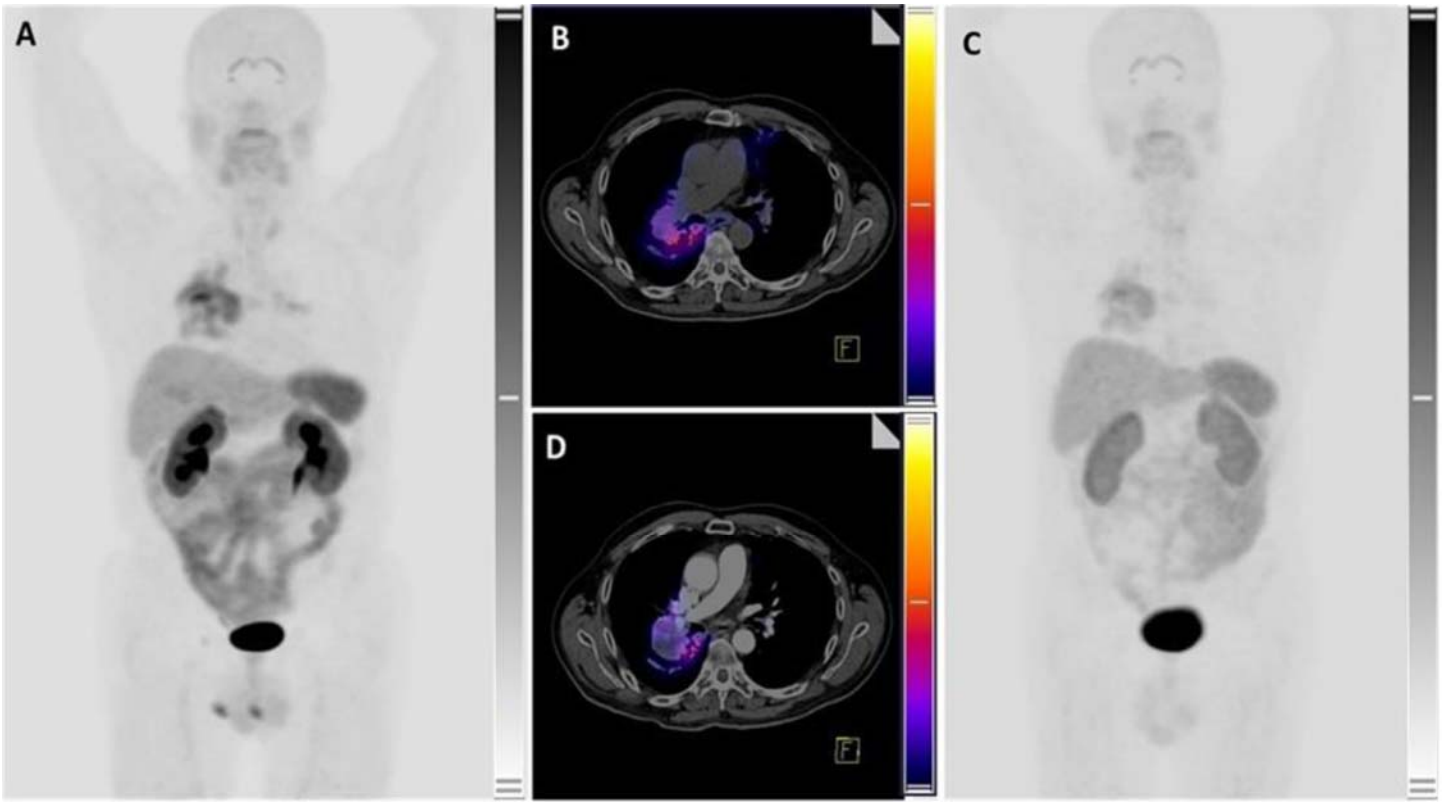

FIGURE 2. Male 62 years with lung adenocarcinoma. The ^{68}Ga-DOTA-E-[c(RGDfk)]^{2} PET / CT (A/B) prior to treatment with multikinase inhibitors shows intense avidity for the radiotracer in the right lung lesion as well as ipsilateral and contralateral mediastinal lymph nodes, tumor volume is 178cm^{3} with SUVmax 7.6. The PET/CT (C/D) post-therapy shows significant reduction of avidity in lung lesion and lymph nodes with tumor volume of 56 cm^{3} and SUVmax of 3.5 (scale 0-10 SUV-bw). The PFS of this patient was 6 months.

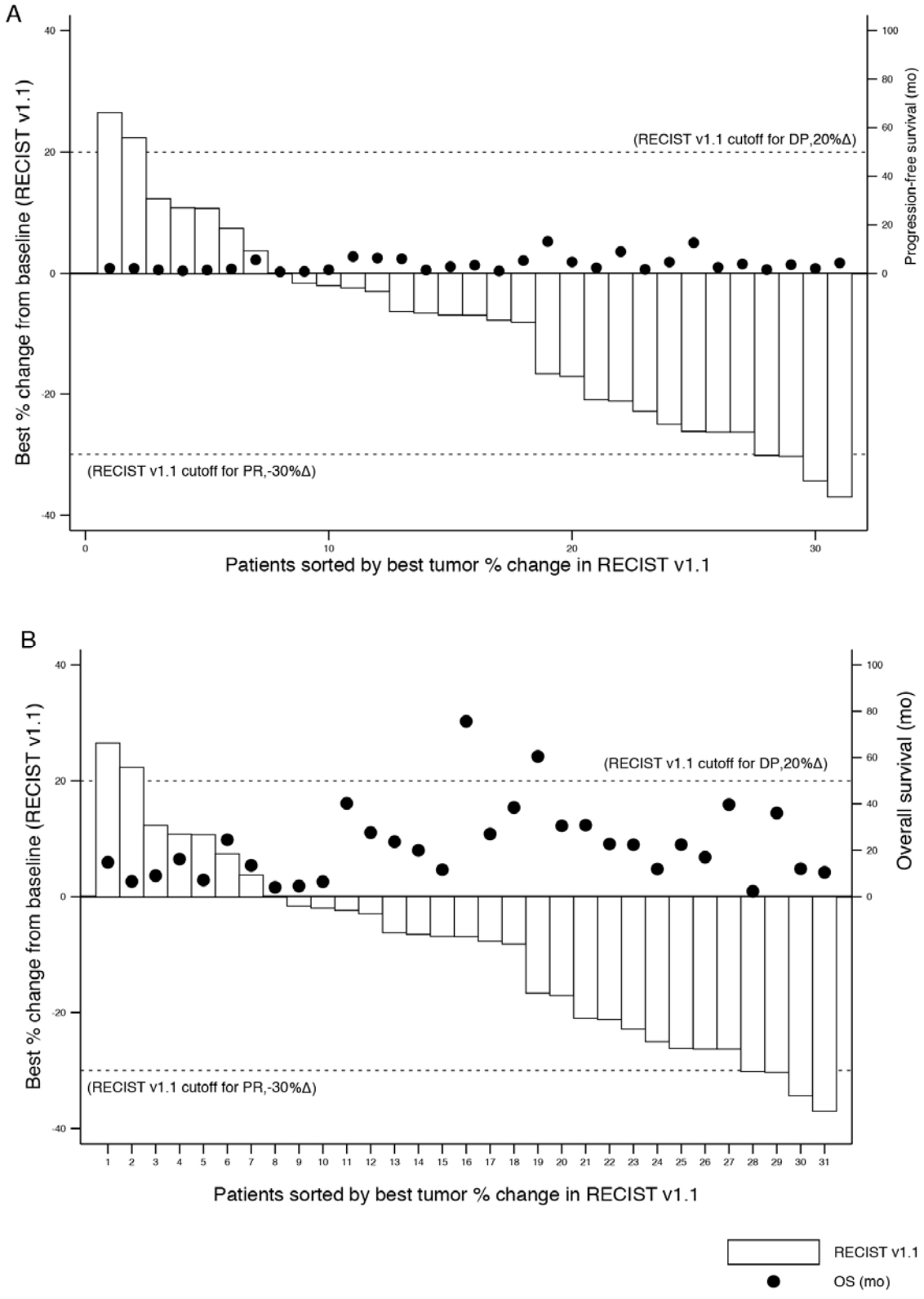

FIGURE 3. Waterfall plots of the percent of change in (A) tumoral volume by RECIST V1.1 and by (B) lung tumor SUVmax uptake measured with ^{68}Ga-DOTA-E-[c(RGDfk)]^{2}PET/CT

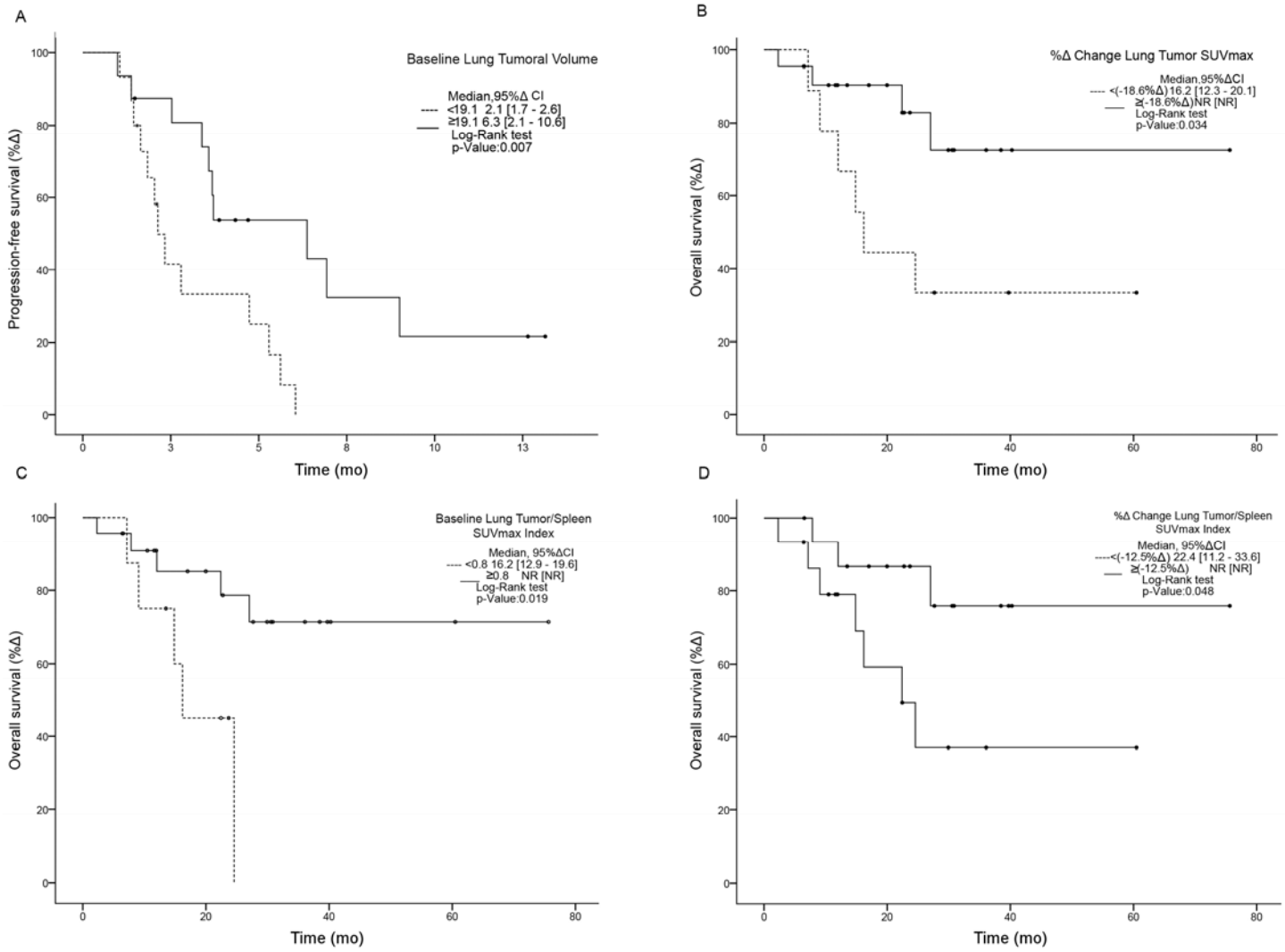

FIGURE 4. Kaplan-Meier curves for significant differences in PFS (A) and OD (B-D)

TABLE 1. Baseline, follow-up and percent change of ^{68}Ga-DOTA-E-[c(RGDfK)]^2 PET/CT and angiogenic soluble factors (N=31)

Parameter	Baseline			Follow-Up			Percent change (% Δ)	Wilcoxon *P*
	Median	Range		Median	Range		Median	
Lung Tumor SUVmax	4.3	1.3	9.2	3.5	1.8	7.8	-18.6	0.188
Spleen SUVmax	5.0	1.6	8.4	5.8	2.4	12.1	16	0.427
Liver SUVmax	3.2	1.0	5.5	3.3	1.6	6.5	3.1	0.666
Lung Tumor/Spleen SUVmax Index	0.8	0.4	1.6	0.7	0.3	1.3	-12.5	**0.022**
Lung Tumor/Liver SUVmax Index	1.4	0.6	2.3	1.2	0.4	2.8	-14.2	0.057
Lung Tumoral Volume	19.1	0.5	557.1	11.9	0	634.4	-37.7	**0.002**
FGF (pg/mL)	39.2	3.2	337	88.1	8.1	297.8	124.7	**0.030**
VEGF (pg/mL)	182.4	1.9	609.2	193.1	23.6	574.4	5.9	0.253
PDGF-AB (pg/mL)	8655.6	2136.1	32150.0	14700.0	1681.9	39038.9	69.8	**0.035**

Abbreviations= PET/CT: Positron Emission Tomography/Computed Tomography; SUV: Standardized Unit Values; FGF: Fibroblast growth factor; VEGF: Vascular Endothelial Growth Factor; PDGF-AB: Platelet derived growth factor-AB. Note: 7 (18.4%) patients were excluded due to missing values at follow-up.

TABLE 1. Baseline, follow-up and percent change of ^{68}Ga-DOTA-E-[c(RGDfK)]^2 PET/CT and angiogenic soluble factors (N=31)

SUPPLEMENTARY FIGURE 1. Overall adverse events.

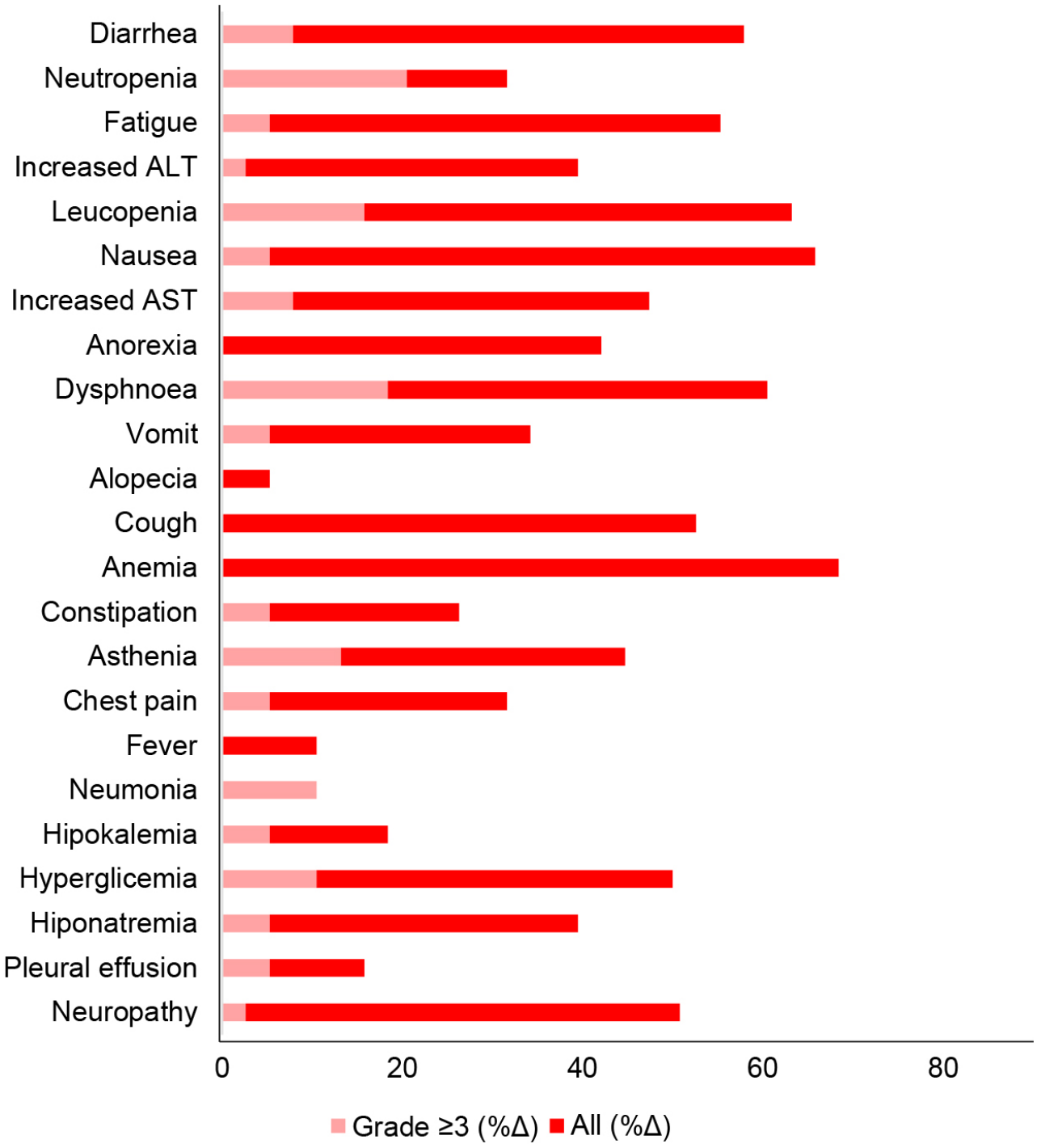

SUPPLEMENTARY FIGURE 2. Scatterplots of the significant correlations among baseline PET/CT parameters measured with ^{68}Ga-DOTA-E-[c(RGDfK)]^2 radiotracer and angiogenic soluble factors.

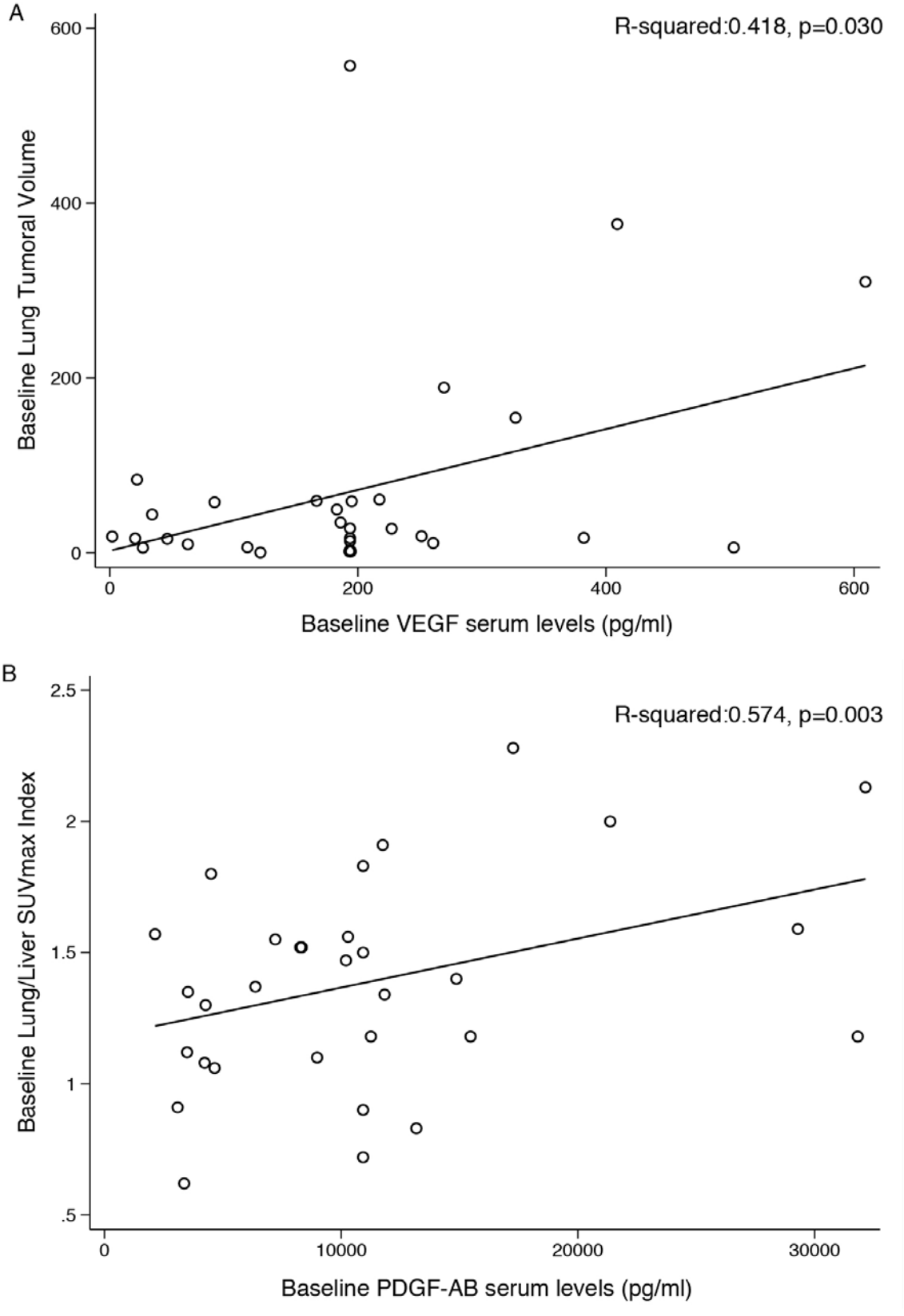

TABLE S1. General characteristics of patients (N=38)	
Variable	% (n/N)
Gender	
Female	65.8 (25/38)
Male	34.2 (13/38)
Age	
Mean ± SD	58.7 ±11.4
≤ 60 yrs	42.1 (16/38)
> 60 yrs	57.9 (22/38)
Tobacco expossure	
Non-smokers	57.9 (22/38)
Smokers	42.1 (16/38)
Tobacco index	
Median (range)	24 (1-102)
Diabetes Mellitus	
Absent	84.2 (32/38)
Present	15.8 (6/38)
Systemic hypertension	
Absent	71.1 (27/38)
Present	28.9 (11/38)
Clinical stage at diagnosis	
II-III	18.4 (7/38)
IV	81.6 (31/38)
Baseline ECOG	
≤1	97.4 (37/38)
≥2	2.6 (1/38)
Adenocarcinoma histological pattern	
Lepidic	5.3 (2/38)
Papillary	15.8 (6/38)
Acinar	21.1 (8/38)
Solid	10.5 (4/38)
Other/Not specified	47.4 (18/38)
Carcinoembrionary antigen	
Median [Range]	7.3 [0.53 - 1,590.0]
Carcinoembrionary antigen	
≤10 pg/mL	52.6 (20/38)
>10 pg/mL	47.4 (18/38)
1st line therapy scheme	
Cis/Carbo-platin /Taxane	71.1 (27/38)
Cis/Carbo-platin /Pemetrexed	23.7 (9/38)
Cis/Carboplatin/ Gemcitabine	5.6 (2/38)
1st line Overall response rate	47.3 (18/38)
1st line Disease control rate	73.7 (28/38)
2nd line therapy scheme	
Nintedanib/Docetaxel	100 (38/38)
2nd line Overall response rate	7.9 (3/38)
2nd line Disease control rate	47.3 (18/38)
Abbreviations= SD: standard deviation; yrs: years; ECOG: Eastern Cooperative Oncology Group of performance status.	

Table S2. Characteristics of patients according to disease control rate (DCR) to nintedanib assessed by ^{68}Ga-DOTA-E-[c(RGDfK)]^2 PET/CT

Variable	Disease control rate (CR + PR + SD)		*P*
	No	Yes	
	% (n/N)	% (n/N)	
Gender			
Female	50.0 (12/24)	50.0 (12/24)	0.715*
Male	40.0 (4/10)	60.0 (6/10)	
Age			
≤ 60 yrs	56.3 (9/16)	43.8 (7/16)	0.311
> 60 yrs	38.9 (7/18)	61.1 (11/18)	
Tobacco exposure			
Non-smokers	42.9 (9/21)	57.1 (12/21)	0.533
Smokers	53.8 (7/13)	46.2 (6/13)	
Diabetes Mellitus			
Absent	48.3 (14/29)	51.7 (15/29)	1.000*
Present	40.0 (2/5)	60.0 (3/5)	
Systemic hypertension			
Absent	56.0 (14/25)	44.0 (11/25)	0.125*
Present	22.2 (2/9)	77.8 (7/9)	
Number of metastases			
≤1	30.0 (3/10)	70.0 (7/10)	0.270*
≥2	54.2 (13/24)	45.8 (11/24)	
Histological grade of differentiation†			
Low & Moderate	35.7 (5/9)	64.3 (9/14)	0.527
High	50.0 (2/4)	50.0 (2/4)	
Not specified	56.3 (9/16)	43.8 (7/16)	
Carcinoembrionary antigen			
≤10 pg/mL	61.1 (11/18)	38.9 (7/18)	0.100
>10 pg/mL	31.3 (5/16)	68.8 (11/16)	

Abbreviations= PET/CT: Positron Emission Tomography/Computed Tomography; CR: complete response; PR: partial response; SD: stable disease; yrs: years. p-Value for Chi-Square test and (*) Fisher´s exact test.
Note: †according to adenocarcinoma IASLC/ATS/ERS classification.

TABLE S3. ^{68}Ga-DOTA-E-[c(RGDfK)]^2 PET/CT parameters (N=30) according to disease control rate

Variable	Disease Control Rate							
	Non-responders				Responders			
	Median	Range		*P*	Median	Range		*P*
Lung Tumor SUVmax								
Baseline	5.5	1.3	7	0.346	4.3	2	9.2	0.363
Follow-Up	4	2.5	6.6		3.5	1.8	7.8	
%Δ Lung Tumor SUVmax		-27.3				-18.6		
Spleen SUVmax								
Baseline	5	1.6	6.9	0.118	5.8	4.3	8.4	0.255
Follow-Up	5.8	2.4	8.3		5.2	2.8	12.1	
%Δ Spleen SUVmax		16				-10.3		
Liver SUVmax								
Baseline	3.5	1	5	0.753	3.2	2.1	5.5	0.410
Follow-Up	3.3	2	5.9		3.1	1.6	6.5	
%Δ Liver SUVmax		-5.7				-3.1		
Lung Tumor/Spleen SUVmax Index								
Baseline	1	0.4	1.6	**0.008**	0.8	0.4	1.1	0.806
Follow-Up	0.7	0.4	1.3		0.7	0.5	1.2	
%Δ Lung/Spleen Index		-30				-13		
LungTumor/Liver SUVmax Index								
Baseline	1.5	0.8	2.3	0.074	1.2	0.6	2.1	0.629
Follow-Up	1.2	0.8	2.8		1.3	0.7	1.9	
%Δ Lung/Liver SUVmax Index		-18				6.8		
Lung Tumoral Volume								
Baseline	49.6	0.5	557.1	0.088	17.2	1.8	189	**0.005**
Follow-Up	35.9	0.3	634.4		10.8	0	180	
%Δ Lung Tumoral Volume		-27.6				-37.2		

Abbreviations= PET/CT: Positron Emission Tomography/Computed Tomography; %Δ: percentage of change; SUV: Standardized Unit Values.

Table S4. Association of ^{68}Ga-DOTA-E-[c(RGDfK)]2 PET/CT parameters with baseline and %Δ angiogenic soluble factors

Variable	Baseline FGF		Baseline VEGF		Baseline PDGF-AB	
PET/CT parameter	r^2	*P*	r^2	*P*	r^2	*P*
Baseline Lung Tumor SUVmax	-0.219	0.316	0.078	0.719	0.339	0.083
Baseline Spleen SUVmax	-0.062	0.779	-0.080	0.710	0.130	0.520
Baseline Liver SUVmax	-0.110	0.617	0.056	0.793	0.128	0.526
Baseline Lung Tumor/Spleen SUVmax Index	-0.208	0.340	0.167	0.435	0.332	0.091
Baseline Lung Tumor/Liver SUVmax Index	-0.173	0.430	0.041	0.848	0.418	**0.030**
Baseline Lung Tumoral Volume	0.113	0.607	0.574	**0.003**	-0.310	0.116

Abbreviations= SUV: Standardized Unit Values; PET/CT: Positron Emission Tomography/Computed Tomography; %Δ: percentage of change; FGF: Fibroblast growth factor; VEGF: Vascular endothelial growth factor; PDGF-AB: Platelet derived growth factor-AB; r2: root-squared.

S5. Univariate analysis of clinical and ^{68}Ga-DOTA-E-[c(RGDfK)]2 PET/CT factors associated with Progression-free Survival and Overall Survival

Variable	Progression-free Survival			Overall Survival		
	Median	95% CI	*P*	Median	95% CI	*P*
Overall	3.7	[2.04 - 5.38]		NR	NR	
Gender						
Female	3.7	[1.01 - 6.34]	0.666	NR	NR	0.726
Male	5.6	[2.24 - 8.98]		NR	NR	
Age						
<60 yrs	3.4	[1.84 - 4.92]	0.307	NR	NR	0.265
>60 yrs	5.6	[2.43 - 8.79]		NR	NR	
Tobacco expossure						
Non-smokers	3.7	[1.16 - 6.19]	0.414	NR	NR	**0.038***
Smokers	5.3	[0.64 - 6.77]		NR	NR	
Diabetes Mellitus						
Absent	3.7	[2.18 - 5.17]	0.555	NR	NR	0.985
Present	5.3	[0.00 - 13.59]		NR	NR	
Systemic hypertension						
Absent	3.4	[1.73 - 5.03]	**0.023**	NR	NR	0.118
Present	6.4	[5.54 - 7.20]		NR	NR	
Clinical stage at diagnosis						
II-III	3.4	[0.00 - 7.34]	0.412	NR	NR	0.734
IV	3.7	[1.37 - 6.04]		NR	NR	
Baseline ECOG						
≤1	3.7	[2.05 - 5.30]	0.431	NR	NR	0.488
≥2	NR	[NR]		NR	NR	
Carcinoembrionary antigen						
≤10 pg/mL	3.7	[1.98-5.37]	0.629	NR	NR	0.972
>10 pg/mL	5.6	[2.29 - 8.94]		NR	NR	
Baseline Lung Tumor SUVmax						
<4.3	4.7	[0.09 - 9.37]	0.600	7.1	NR	0.170
≥4.3	3.7	[3.15 - 4.20]		NR	NR	
%Δ Lung Tumor SUVmax						
< - 18.6	2.0	[1.46 - 2.61]	0.120*	7.1	[0.0 - 14.7]	**0.016**
≥ - 18.6	3.7	[2.24 - 5.17]		NR	NR	
Baseline Spleen SUVmax						
<5	4.7	[2.30 - 7.15]	0.618	NR	NR	0.888
≥5	3.6	[2.25 - 4.90]		NR	NR	
%Δ Spleen SUVmax						
< 16.0	4.7	[0.73 - 8.72]	0.790	NR	NR	0.603
≥ 16.0	3.6	[2.39 - 4.77]		NR	NR	
Baseline Liver SUVmax						
<3.2	4.7	[0.44 - 9.01]	0.673	NR	NR	0.697
≥3.2	3.7	[2.11 - 5.24]		NR	NR	
%Δ Liver SUVmax						
< 3.5	4.7	[0.69-8.77]	0.858*	NR	NR	0.069*

≥ 3.5	3.6	[2.27 - 4.88]		NR	NR	
Baseline Lung Tumor/Spleen SUVmax Index						
<0.8	2.8	[0.87 - 4.71]	0.460	4.6	[1.4 - 7.7]	0.022
≥0.8	3.7	[1.37 - 6.04]		NR	NR	
%Δ Lung Tumor/Spleen SUVmax Index						
< - 12.5	2.8	[0.33 - 5.24]	0.409*	7.8	[5.9 - 9.8]	**0.043**
≥ -12.5	4.7	[2.52 - 6.93]		NR	NR	
Baseline Lung Tumor/Liver SUVmax Index						
<1.4	2.3	[0.00 - 5.34]	0.464*	NR	NR	0.486
≥1.4	3.7	[3.12 - 4.30]		NR	NR	
%Δ Lung Tumor/Liver SUVmax Index						
< -14.2	3.7	[1.77 - 5.58]	0.308	NR	NR	0.343
≥ -14.2	3.7	[1.55 - 5.87]		NR	NR	
Baseline Lung Tumoral Volume						
<19.1	2.1	[1.66 - 2.61]	**0.007**	NR	NR	0.459
≥19.1	6.4	[2.12 - 10.62]		NR	NR	
%Δ Lung Tumoral Volume						
< -37.7	3.7	[2.32 - 5.03]	0.365	NR	NR	0.378
≥ -37.7	2.8	[0.67 - 4.91]		NR	NR	

Abreviations: CI: Confidence interval; yrs:years, ECOG PS: European Clinical Oncological Group performance status; SUV: Standarized Unit Values; %Δ: percentage of change. Notes (*) Breslow test.

TABLE S6. Multivariate analysis of clinical and ^{68}Ga-DOTA-E-[c(RGDfK)]^2 PET/CT factors associated with Progression-free Survival and Overall Survival

Variable	Progression-free Survival		Overall Survival	
	HR (95% CI)	*P*	HR (95% CI)	*P*
Gender			0.9 (0.27 - 3.53)	0.979
Age			1.4 (0.55 - 3.67)	0.455
Tobacco expossure			2.3 (0.68 - 7.95)	0.176
Systemic hypertension	0.2 (0.07 - 0.80)	**0.021**		
%Δ Lung Tumor SUVmax			3.1 (1.0 - 9.8)	**0.048**
Baseline Spleen SUVmax	0.4 (0.14 - 1.09)	0.074		
Baseline Lung Tumoral Volume	0.4 (0.17 - 1.08)	0.075		

Abbreviations= PET/CT: Positron Emission Tomography/Computed Tomography; CI: Confidence Interval; %Δ: percentage of change; SUV: Standardized Unit Values.